THE BELL SYSTEM TECHNICAL JOURNAL
Vol. 59, No. 8, October 1980
Printed in U.S.A.

Computation of the Frequency Response of a Class of Symmetric *N*-Way Power Dividers

By A. A. M. SALEH

(Manuscript received April 9, 1980)

Symmetric n-way power dividers (and combiners) are needed to feed multi-element antennas and to combine the output powers of a number of solid-state amplifiers and oscillators over a broad frequency range. We present a unified method of analysis for computing the frequency responses of symmetric, n-way power dividers of the Wilkinson, radial, and fork types, whose transmission lines are allowed to be coupled and nonuniform and may be surrounded by an inhomogeneous dielectric medium. The method is based on the analysis of a simple one- or two-port network for each of the n eigenmodes of the power-divider structure, resulting in a considerable improvement in the speed of computation, as well as a sizable reduction in storage requirements, as compared to a standard method of nodal analysis. Furthermore, the aforementioned one- and two-port networks facilitate the design and optimization of the power dividers over a desired frequency band.

I. INTRODUCTION

Symmetric, n-way power dividers have the advantage of giving neither amplitude nor phase power-division unbalance at all frequencies. Thus, they are used in many broadband applications such as in the feed system of multi-element antennas, and as combiners of solid-state amplifiers and oscillators. They are also used (without isolation resistors) for fanning in and fanning out in high-speed, digital integrated circuits. This paper is primarily concerned with methods of analysis suitable for the computation of the frequency response of the class of symmetric, n-way power dividers represented schematically in Fig. 1. This includes the well-known Wilkinson power divider,[1-8] the recently introduced radial[9-12] and fork[12,13] power dividers (see also Ref. 14, Fig. 1), and the coaxial power divider described in Ref. 14, Fig. 2, which has the same topology as the radial power divider. The radial

and the fork power dividers are particularly interesting since they are both planar.

When Wilkinson[1] introduced his power divider, which consisted of one stage of n, uniform, uncoupled transmission lines, and one network of isolation resistors, he limited his analysis to the center frequency. Later, several simple methods of analysis were introduced for the computation of the frequency response of single- or multi-stage, Wilkinson, n-way power dividers with uniform, uncoupled lines and an arbitrary n,[2-4] with uniform uncoupled lines and $n = 2$,[5] with uniform, coupled lines and $n = 2$,[6] with nonuniform, uncoupled lines and $n = 2$,[7] and with uniform, coupled lines and $n = 3$.[8] No methods are available in the literature for the analysis of Wilkinson power dividers with coupled and/or nonuniform transmission lines and an arbitrary value of n.

The author[12] presented a method of analysis that led to closed-form expressions for the scattering parameters of single- and double-stage, radial and fork, n-way power dividers, and gave general design formulas and tables for the values of the isolation resistances and characteristic impedances involved to optimize the match and isolation among their output ports. That work, however, was limited to the center frequency and was restricted to uniform lines that may include coupling only in the first stage.

A unified method of analysis is presented in the present paper for the computation of the frequency responses of multi-stage, Wilkinson, radial, and fork n-way power dividers. The n-conductor transmission lines employed in these power dividers may be coupled and nonuniform and may be surrounded by an inhomogeneous dielectric medium. The method is based on developing n simple one- and two-port networks that correspond to the n eigenmodes of the power-divider structure. Nagai, Maekawa and Ono[14] used similar networks but gave no details of their development. (See note at the end of paper.)

II. GEOMETRY AND BASIC ASSUMPTIONS

A schematic diagram of an n-way, equi-amplitude, equi-phase power divider of the type considered in this paper is shown in Fig. 1. A source of admittance Y_S is connected to the input port (port 0), and n identical loads of admittance Y_L are connected to the output ports (ports 1 through n). The power divider has two main sections. The first section is an input transformer consisting of p cascaded stages of transmission lines of characteristic admittances Y_k', and electrical lengths ϕ_k', $k = 1, 2, \cdots, p$. The second section consists of l stages of n-conductor transmission lines, within a shield or over a ground plane, with a floating, n-terminal network of isolation resistors connected at the output end of each stage. Three different geometries for these networks

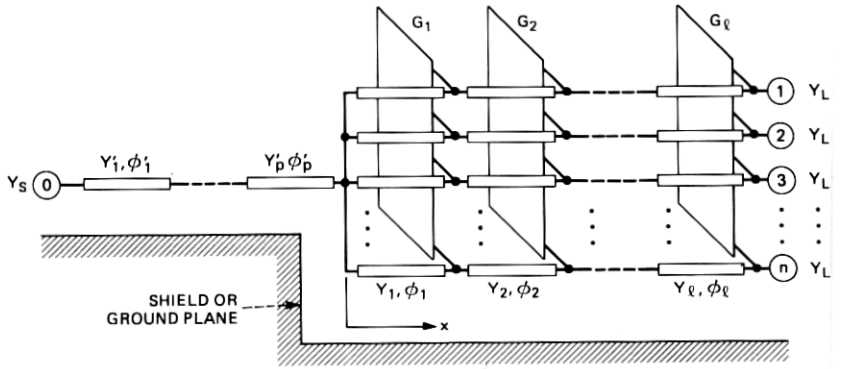

Fig. 1—A schematic diagram of an l-stage, n-way power divider with a p-stage input transformer. The G's are isolation-resistor networks (see Fig. 2).

are shown in Fig. 2, which correspond to (a) the Wilkinson power divider,[1-8] (b) the radial power divider[9-12] or to the coaxial power divider described in Ref. 14, Fig. 2, and (c) the fork power divider[12,13] (see also Ref. 14, Fig. 1). All the isolation resistors in each stage, $k = 1, 2, \cdots, l$, have the same conductance, G_k, which may be different for different stages. Thus, the conductance matrices of the isolation-resistor networks may be written as

$$\mathbf{G}_k = G_k\mathbf{M}, \qquad k = 1, 2, \cdots, l, \tag{1}$$

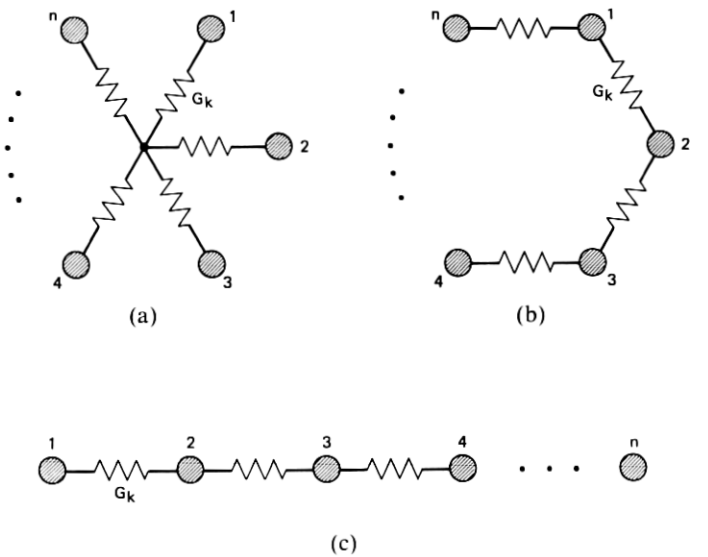

Fig. 2—Three different geometries for the isolation-resistor networks of Fig. 1, corresponding to the Wilkinson (a), the radial (b), and the fork (c) power dividers. The conductance of each isolation resistor is G_k, where k (= 1, 2, $\cdots$, l) is the stage number.

where $\mathbf{M}$ is an $n \times n$ matrix that depends on the topology of the isolation resistors and is independent of k. A q-stage output transformer may be included at each output port by eliminating the isolation-resistor networks, i.e., by setting $G_k = 0$, in the last q stages.

Each of the n-conductor transmission-line stages may consist of electrically identical, coupled or uncoupled, longitudinally uniform or nonuniform conductors in a transversely homogeneous or inhomogeneous dielectric medium. However, to ensure proper operation of the power divider and to facilitate the method of analysis presented in this paper, these transmission lines, and the isolation-resistor networks, must satisfy the three basic assumptions given below. As is seen later, these assumptions are not as restrictive as may appear at a first glance. For example, they are automatically satisfied when the n conductors are identical and uncoupled from one another, or when the arrangement of the n conductors, which may be arbitrarily coupled, and the geometry of the isolation-resistor networks are both circularly symmetric, as is the case in the Wilkinson and the radial power dividers. Also, in a planar, side-by-side conductor arrangement combined with a linear geometry for the isolation-resistor networks, as is the case in the fork power divider, these assumptions can be satisfied after imposing some realistic conditions, which are discussed later.

Let $\mathbf{C}_k(x)$ and $\bar{\mathbf{C}}_k(x)$ be, respectively, the $n \times n$ per-unit-length (PUL) capacitance matrices[15] of the n conductors at a location x on the kth stage when the surrounding dielectric, if any, is left in place, and when it is replaced by free space. Various numerical methods are available in the literature[16–18] for the computation of the PUL capacitance matrices of uniform coupled or uncoupled lines in a homogeneous or inhomogeneous dielectric medium. The same methods can be used for lines with gradual nonuniformities by considering them to be locally uniform in the vicinity of any given cross section.

Assumption 1: The matrices $\mathbf{C}_k(x)$ and $\bar{\mathbf{C}}_k(x)$ have the same set of real, orthonormal eigenvectors, $\mathbf{q}_m$, $m = 0, 1, \cdots, n-1$, which are independent of both k and x, even for nonuniform lines.

Thus, for $k = 1, 2, \cdots, l$, and $m = 0, 1, \cdots, n-1$,

$$\mathbf{C}_k(x)\mathbf{q}_m = \eta_{k,m}(x)\mathbf{q}_m, \tag{2a}$$

$$\bar{\mathbf{C}}_k(x)\mathbf{q}_m = \bar{\eta}_{k,m}(x)\mathbf{q}_m, \tag{2b}$$

where the eigenvalues, $\eta_{k,m}(x)$ and $\bar{\eta}_{k,m}(x)$, are real and positive since the PUL capacitance matrices are real, symmetric and positive definite.[15]

Assumption 2: One of the aforementioned eigenvectors, whose mode

number is defined to be $m = 0$, is the vector

$$\mathbf{q}_0 = n^{-1/2}\begin{bmatrix} 1 \\ 1 \\ \vdots \\ 1 \end{bmatrix}. \tag{3}$$

Since the sum of the ith row of the PUL capacitance matrix is the PUL capacitance to ground of the ith conductor,[15] it follows from (2) and (3) that Assumption 2 is equivalent to requiring all conductors to have the same PUL capacitance to ground at each cross section. An important implication of this assumption in the case of uncoupled lines, where both $\mathbf{C}_k(x)$ and $\bar{\mathbf{C}}_k(x)$ are diagonal, is that each matrix would have equal diagonal elements, and hence, equal eigenvalues; i.e., both $\eta_{k,m}(x)$ and $\bar{\eta}_{k,m}(x)$ become independent of m. In that case, the set of eigenvectors of both matrices is arbitrary.

Assumption 3: All conductance matrices, $\mathbf{G}_k$, of the isolation-resistor networks have the same set of eigenvectors, which coincide with the set of real, orthonormal vectors defined in Assumption 1.

Thus, from (1),

$$\mathbf{M}\mathbf{q}_m = \lambda_m \mathbf{q}_m, \qquad m = 0, 1, \cdots, n-1, \tag{4}$$

where the eigenvalues, λ_m, are real nonnegative numbers because the conductance matrices of passive, resistive networks are real, symmetric, and positive semidefinite.

Since no current would flow in the terminals of an isolation-resistor network when the voltages between its terminals and ground are all equal, it follows that the multiplication of the matrix $\mathbf{G}_k$, or $\mathbf{M}$, by a voltage vector proportional to $\mathbf{q}_0$, defined in (3), results in the zero vector. Thus, $\mathbf{q}_0$ is indeed an eigenvector of $\mathbf{M}$, with the corresponding eigenvalue

$$\lambda_0 = 0. \tag{5}$$

As will be seen later, the above three assumptions guarantee that the power-divider structure can support n *uncoupled* modes, one for each $\mathbf{q}_m$. Furthermore, the mode associated with $\mathbf{q}_0$, given in (3), is the common, or equal-voltage, equal-current mode, which ensures equi-amplitude, equi-phase power division at all frequencies with no dissipation in the isolation resistors, when a signal is applied to the input port of the power divider.

III. EIGENMODES IN THE *N*-CONDUCTOR TRANSMISSION LINES

Under the quasi-static, or quasi-TEM approximation, the generalized, lossless, telegrapher's equations, with $\exp(j\omega t)$ excitation, for any stage

of the n-conductor transmission lines in Fig. 1 assume the form[15]

$$\frac{d}{dx}\mathbf{I}_k(x) = -j\omega\mathbf{C}_k(x)\mathbf{V}_k(x), \tag{6a}$$

$$\bar{\mathbf{C}}_k(x)\frac{d}{dx}\mathbf{V}_k(x) = -j(\omega/c^2)\mathbf{I}_k(x), \tag{6b}$$

where k $(= 1, 2, \cdots, l)$ is the stage number, x is the distance along the stage, ω is the angular frequency, c is the speed of light in free space, $\mathbf{V}_k(x)$ and $\mathbf{I}_k(x)$ are $n \times 1$ vectors representing, respectively, the voltages and currents on the n conductors, and $\mathbf{C}_k(x)$ and $\bar{\mathbf{C}}_k(x)$ are the $n \times n$, PUL capacitance matrices defined in the previous section.

It follows from (2) and (6) that the voltage and current eigenvectors associated with the mth mode in the kth stage can be written as

$$\mathbf{V}_{k,m}(x) = v_{k,m}(x)\mathbf{q}_m, \tag{7a}$$

$$\mathbf{I}_{k,m}(x) = i_{k,m}(x)\mathbf{q}_m, \tag{7b}$$

where $v_{k,m}(x)$ and $i_{k,m}(x)$ are scaler functions satisfying the transmission-line differential equations

$$\frac{d}{dx}i_{k,m}(x) = -j\beta_{k,m}(x)Y_{k,m}(x)v_{k,m}(x), \tag{8a}$$

$$\frac{d}{dx}v_{k,m}(x) = -j[\beta_{k,m}(x)/Y_{k,m}(x)]i_{k,m}(x), \tag{8b}$$

where we defined the modal characteristic admittance

$$Y_{k,m}(x) \equiv c[\eta_{k,m}(x)\bar{\eta}_{k,m}(x)]^{1/2} \tag{9a}$$

and the modal propagation constant

$$\beta_{k,m}(x) \equiv (\omega/c)[\eta_{k,m}(x)/\bar{\eta}_{k,m}(x)]^{1/2}. \tag{9b}$$

Note that if the surrounding dielectric medium is homogeneous of permitivity ϵ_k, then $\mathbf{C}_k(x) = \epsilon_k\bar{\mathbf{C}}_k(x)$ and hence $\eta_{k,m}(x) = \epsilon_k\bar{\eta}_{k,m}(x)$. Thus, (9b) gives $\beta_{k,m}(x) = (\omega/c)\sqrt{\epsilon_k}$, which is independent of m and x, even for nonuniform and/or coupled lines.

3.1 Uniform lines

If the kth stage of the n-conductor lines is uniform, or even if it is nonuniform with the cross section at any distance being a scaled version of that at any other distance, then $\mathbf{C}_k$ and $\bar{\mathbf{C}}_k$, and hence also $\eta_{k,m}$ and $\bar{\eta}_{k,m}$, are independent of x. In that case, (8) and (9) indicate that the mth mode is represented in the kth stage by a uniform transmission line of characteristic admittance

$$Y_{k,m} = c(\eta_{k,m}\bar{\eta}_{k,m})^{1/2} \tag{10a}$$

and electrical length

$$\phi_{k,m} = \beta_{k,m} L_k = (\omega/c)(\eta_{k,m}/\bar{\eta}_{k,m})^{1/2} L_k, \tag{10b}$$

where L_k is the length of the kth stage. If, in addition to being uniform, the lines are also uncoupled, it follows from (10) and from the discussion following Assumption 2 that $Y_{k,m} = Y_k$ and $\phi_{k,m} = \phi_k$ are independent of m. In that case, Y_k and ϕ_k are simply the characteristic admittance and electrical length of each line in the kth stage.

3.2 Nonuniform lines

For some special cases of nonuniform lines, (8) can be solved analytically (see, for example, the fundamental-mode solution of radial waveguides given in Ref. 19). However, in the general case of nonuniform lines, (8) has to be solved numerically for each mode and each stage. An effective numerical method of solution is to approximate the nonuniform transmission line represented in (8) by a cascade of a large number, s, of small, piecewise uniform, transmission-line segments of lengths Δ_i, $i = 1, 2, \cdots, s$. In that case, the $ABCD$ matrix of the mth mode on the kth stage is calculated from the matrix product

$$\begin{bmatrix} A_{k,m} B_{k,m} \\ C_{k,m} D_{k,m} \end{bmatrix} \approx \prod_{i=1}^{i=s} \begin{bmatrix} \cos[\beta_{k,m}(x_i)\Delta_i] & jY_{k,m}^{-1}(x)\sin[\beta_{k,m}(x_i)\Delta_i] \\ jY_{k,m}(x)\sin[\beta_{k,m}(x_i)\Delta_i] & \cos[\beta_{k,m}(x_i)\Delta_i] \end{bmatrix}, \tag{11}$$

where x_i is the location of the center of the ith segment. The m may be dropped from (11) if the lines are uncoupled.

IV. DEVELOPING THE MODAL EQUIVALENT CIRCUITS

In this section, we show that the power divider of Fig. 1 can be represented by n simple networks—one lossless two-port network (Fig. 3a) corresponding to the common mode ($m = 0$), and $n - 1$, generally lossy, one-port networks (Fig. 3b) corresponding to the remaining modes ($m = 1, 2, \cdots, n - 1$).

A mode, m, on the n-conductor lines is identified from the fact that both its voltage and current vectors are proportional to $\mathbf{q}_m$ everywhere, as given by (7). If the n-conductor lines are uniform, the mth mode is represented on the kth stage by a uniform transmission line of characteristic admittance $Y_{k,m}$, given by (10a), and electrical length $\phi_{k,m}$, given by (10b), as depicted in Fig. 3. If the n-conductor lines are nonuniform, then the corresponding transmission lines in Fig. 3 should be replaced by nonuniform lines whose $ABCD$ matrices are given by (11).

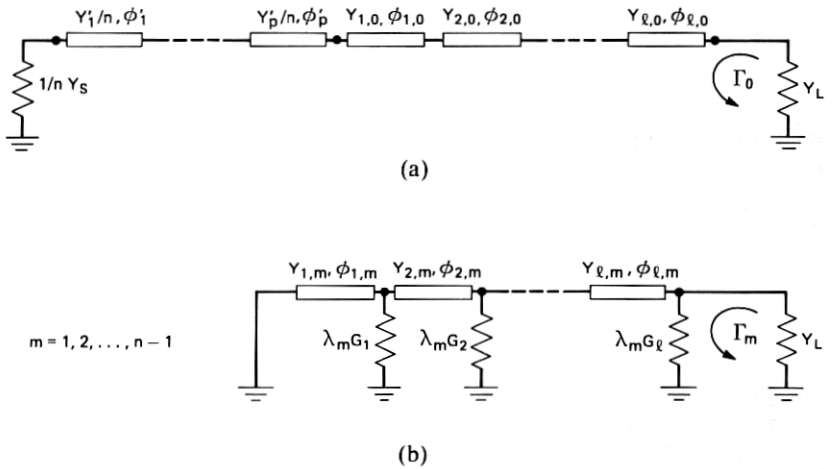

Fig. 3—Equivalent circuits for the n modes of the power divider of Fig. 1, corresponding to (a) the common mode, $m = 0$, and (b) the remaining modes.

Since each $\mathbf{q}_m$ is an eigenvector of every $\mathbf{G}_k$, as given by Assumption 3, it follows that if a voltage vector proportional to $\mathbf{q}_m$ is applied to any isolation-resistor network, then the corresponding current vector is also proportional to $\mathbf{q}_m$. Thus, the isolation-resistor networks preserve each of the modes of the n-conductor lines. Furthermore, it follows from (1) and (4) that the kth isolation-resistor network presents a shunt conductance of $\lambda_m G_k$ to the mth mode, as shown in Fig. 3b. No such conductances exist in Fig. 3a since $\lambda_0 = 0$, as given by (5).

The voltages on all conductors are forced to be equal at the node joining the input transformer and the n-conductor lines in Fig. 1. Since the common mode, $m = 0$, is the only mode with equal voltages on the n conductors, and since all the other modes are orthogonal to that mode, it follows that the common mode is the only mode coupled to the input section of the power divider, as shown in Fig. 3a. The remaining modes are effectively short-circuited at that point, as shown on the left-hand side of Fig. 3b. The $1/n$ factor multiplying the admittances of the input section in Fig. 3a is due to the fact that the current at the output end of the input transformer is equally divided among the n conductors of the output section.

Since the load admittances of the power divider are all equal to Y_L, it follows that the admittance matrix representing these loads is diagonal, with all its diagonal elements equal to Y_L. Thus, its eigenvectors are arbitrary, and hence can be the set, $\mathbf{q}_m$, $m = 0, 1, \cdots, n-1$, and its eigenvalues are all equal to Y_L. This results in equal, uncoupled loads, Y_L, for all the modal equivalent circuits in Fig. 3.

For $n = 2$, the equivalent circuits in Figs. 3a and 3b coincide,

respectively, with the familiar even-mode and odd-mode circuits used in the analysis of symmetric 2-way power dividers.[5-7]

V. CALCULATION OF THE FREQUENCY RESPONSE

Define the following reflection and transmission coefficients:

r_0: Reflection coefficient of the input port of the two-port network of Fig. 3a.

t_0: Transmission coefficient of the two-port network of Fig. 3a, normalized to the port admittances such that $|t_0|^2$ is the power transmission coefficient.

Γ_m: Reflection coefficient of the output port of the network in Fig. 3 corresponding to the mth mode, $m = 0, 1, \cdots, n-1$.

These coefficients can be calculated at any frequency through the use of standard, *ABCD*-matrix analysis[20] of the one- and two-port networks of Fig. 3. Here, we show how to use this information to calculate the frequency responses of the various elements of the $(n+1) \times (n+1)$ scattering matrix, $\mathbf{S}'$, of the power divider of Fig. 1. Let $\mathbf{S}'$ be put in the partitioned form

$$\mathbf{S}' = \left[\begin{array}{c|ccc} S_{00} & S_{01} & \cdots & S_{0n} \\ \hline S_{01} & & & \\ \vdots & & \mathbf{S} & \\ S_{0n} & & & \end{array}\right], \tag{12}$$

where S_{00} is the reflection coefficient of the input port, S_{0i}, $i = 1, 2, \cdots, n$, are the normalized transmission coefficients between the input port and the n output ports, and $\mathbf{S} = [S_{ij}, i, j = 1, 2, \cdots, n]$ is the symmetric $n \times n$ scattering matrix among the n output ports.

Since the common mode, $m = 0$, is the only mode excited when a signal is applied to the input port of the power divider, it can be shown that

$$S_{00} = r_0 \tag{13}$$

$$S_{0i} = n^{-1/2} t_0, \qquad i = 1, 2, \cdots, n. \tag{14}$$

It follows from losslessness of the network of Fig. 3a that

$$|r_0|^2 + |t_0|^2 = |S_{00}|^2 + n|S_{0i}|^2 = 1. \tag{15}$$

To calculate the output-ports scattering matrix, $\mathbf{S}$, let $\mathbf{a}_m$ and $\mathbf{b}_m$ $(= \mathbf{S}\mathbf{a}_m)$ be the $n \times 1$ vectors representing, respectively, the incident and reflected wave amplitudes at the output ports of the power divider,

corresponding to the mth mode. Thus, from the definition of Γ_m, it follows that $\mathbf{b}_m = \Gamma_m \mathbf{a}_m$. Furthermore, because of (7), and from the fact that $\mathbf{a}_m$ and $\mathbf{b}_m$ are defined by linear combinations of the voltage and current vectors at the output ports, it follows that $\mathbf{a}_m$ and $\mathbf{b}_m$ are both proportional to $\mathbf{q}_m$. Hence, we reach the interesting result that $\mathbf{q}_m$ is an eigenvector of $\mathbf{S}$, with the corresponding eigenvalue Γ_m, for $m = 0, 1, \cdots, n-1$. Thus, defining the orthogonal, modal matrix

$$\mathbf{Q} \equiv [\mathbf{q}_0 \mathbf{q}_1 \cdots \mathbf{q}_{n-1}], \tag{16}$$

and the diagonal matrix of eigenvalues

$$\Gamma = \text{diag}(\Gamma_0, \Gamma_1, \cdots, \Gamma_{n-1}), \tag{17}$$

one can write $\mathbf{S}$ in the form

$$\mathbf{S} = \mathbf{Q}\Gamma\mathbf{Q}^T, \tag{18}$$

where "T" represents matrix transposition. If $q_{m,i}$ is the ith entry of $\mathbf{q}_m$, (18) can be rewritten as

$$S_{ij} = S_{ji} = n^{-1}\Gamma_0 + \sum_{m=1}^{n-1} q_{m,i} q_{m,j} \Gamma_m, \qquad i, j = 1, 2, \cdots, n, \tag{19}$$

where use was made of (3).

VI. THE WILKINSON AND THE RADIAL POWER DIVIDERS

The Wilkinson and the radial power dividers, as well as the coaxial power divider described in Ref. 14, Fig. 2, share the property of circular symmetry. An example of the cross section of their n-conductor lines is given in Fig. 4a, which also shows the various PUL capacitances. Of course, this figure is only a topological representation of the case of radial power dividers, where the actual cross section would lie on the surface of a circular cylinder. Let $C_{k,0}(x)$ be the PUL capacitance to ground of each conductor, and $C_{k,s}(x)$ be the PUL capacitance between two conductors separated by s spaces along the circumference, $s = 1, 2, \cdots, n-1$, where k represents the stage number and x the distance along the stage. Thus, the off-diagonal elements of the PUL capacitance matrix, $\mathbf{C}_k(x)$, are given by

$$\mathbf{C}_k(x)|_{ij} = \mathbf{C}_k(x)|_{ji} = -C_{k,|i-j|}(x) = -C_{k,n-|i-j|}(x),$$

$$i \neq j = 1, 2, \cdots, n, \tag{20a}$$

where the last equality follows from circular symmetry, and its diagonal elements are given by

$$\mathbf{C}_k(x)|_{ii} = C_{k,0}(x) + 2 \sum_{s=1}^{[n/2]} u_s C_{k,s}(x), \qquad i = 1, 2, \cdots, n, \tag{20b}$$

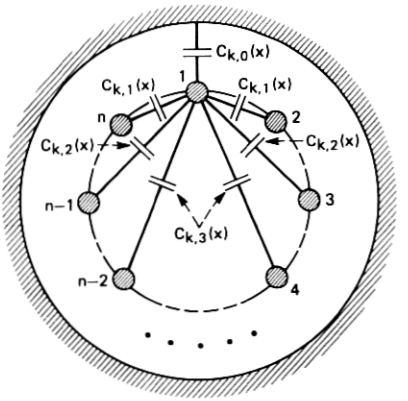

(a)

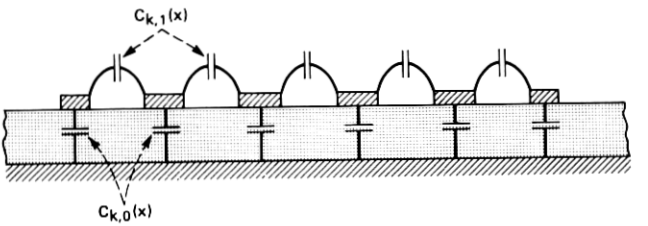

(b)

Fig. 4—Circularly symmetric (a), and side-by-side (b) conductor arrangements. (a) corresponds to the Wilkinson power divider and, topologically, to the radial power divider. (b) corresponds to the fork power divider.

where $[n/2]$ is the integer part of $n/2$, and

$$u_s \equiv \begin{cases} \frac{1}{2}, & n \text{ even}, \quad s = n/2, \\ 1, & \text{otherwise}. \end{cases} \tag{21}$$

Similar expressions hold for the free-space PUL capacitance matrix, $\bar{\mathbf{C}}_k(x)$. The conductance matrix, $\mathbf{G}_k$, of the kth isolation-resistor network is given by (1), with

$$\mathbf{M} = \begin{bmatrix} 1 & 0 & \cdots & 0 \\ 0 & 1 & \cdots & 0 \\ \vdots & \vdots & & \vdots \\ 0 & 0 & \cdots & 1 \end{bmatrix} - \frac{1}{n} \begin{bmatrix} 1 & 1 & \cdots & 1 \\ 1 & 1 & \cdots & 1 \\ \vdots & \vdots & & \vdots \\ 1 & 1 & \cdots & 1 \end{bmatrix} \tag{22}$$

for the resistors configuration of the Wilkinson power divider shown

in Fig. 2a, or

$$\mathbf{M} = \begin{bmatrix} 2 & -1 & & & & & -1 \\ -1 & 2 & -1 & & & 0 & \\ & -1 & 2 & & & & \\ & & & \ddots & & & \\ & & & & 2 & -1 & \\ & 0 & & & -1 & 2 & \\ -1 & & & & & & \end{bmatrix} \tag{23}$$

for the resistor configuration of the radial power divider shown in Fig. 2b.

The matrices $\mathbf{C}_k(x)$, $\bar{\mathbf{C}}_k(x)$, and $\mathbf{M}$ given above are real, symmetric *circulants*,[21] which is a direct consequence of circular symmetry. Including the properties of realness and symmetry to the results given in Ref. 21 for circulants, one can show that all real, symmetric circulants of order n have the same set of real, orthonormal eigenvectors, $\mathbf{q}_m$, $m = 0, 1, \cdots, n-1$, where the ith entry, $i = 1, 2, \cdots, n$, of $\mathbf{q}_m$ is given by

$$q_{m,i} = \begin{cases} n^{-1/2} & m = 0, \\ (2u_m/n)^{1/2}\cos[2m(i-1)\pi/n], & \\ & m = 1, 2, \cdots, [n/2], \\ (2/n)^{1/2}\sin[2m(i-1)\pi/n], & \\ & m = [n/2]+1, [n/2]+2, \cdots, n-1, \end{cases} \tag{24}$$

where u_m is defined in (21) with s replaced by m. Note that (3) is satisfied. Thus, circularly symmetric power dividers automatically satisfy Assumptions 1 to 3 of Section II.

The eigenvalues of $\mathbf{C}_k(x)$ are given, from (2a), (20), and (24), by

$$\eta_{k,0}(x) = C_{k,0}(x), \tag{25a}$$

$$\eta_{k,m}(x) = \eta_{k,n-m}(x) = C_{k,0}(x) + 4\sum_{s=1}^{[n/2]} u_s C_{k,s}(x)\sin^2(ms\pi/n), \quad m = 1, 2, \cdots, n-1. \tag{25b}$$

Similar expressions hold for $\bar{\eta}_{k,m}(x)$.

The eigenvalues of $\mathbf{M}$ for the Wilkinson power divider are given, from (4), (22), and (24), by

$$\lambda_m = 1, \qquad m = 1, 2, \cdots, n-1. \tag{26}$$

The eigenvalues of $\mathbf{M}$ for the radial power divider are given, from (4),

(23), and (24), by

$$\lambda_m = \lambda_{n-m} = 4 \sin^2(m\pi/n), \qquad m = 1, 2, \cdots, n-1. \tag{27}$$

For both power dividers, $\lambda_0 = 0$, as given in (5).

Because of the degeneracies of the mth and $(n-m)$th eigenvalues, $m \neq 0$, shown in (25b), (26), and (27), which can actually be shown to be a property of all real, symmetric circulants, it follows that the modal equivalent circuits of Fig. 3b are identical for the mth and the $(n-m)$th modes. Thus, for the Wilkinson and radial power dividers,

$$\Gamma_m = \Gamma_{n-m}, \qquad m = 1, 2, \cdots, n-1, \tag{28}$$

and, hence, (19) and (24) give

$$S_{ij} = S_{ji} = n^{-1}\left\{\Gamma_0 + 2\sum_{m=1}^{[n/2]} u_m \cos[2m(i-j)\pi/n]\Gamma_m\right\}. \tag{29}$$

Note that S_{ij} is only a function of $|i-j|$, and does not change when $|i-j|$ is replaced by $n-|i-j|$. This, of course, is consistent with the circular symmetry of these power dividers.

For a Wilkinson power divider with *uncoupled* lines, i.e., with $C_{k,s}(x) = 0$ for $s \neq 0$, it follows from (25) that $\eta_{k,m}(x)$ is independent of m. This fact and (26) indicate that the modal equivalent circuits of Fig. 3b are identical for all modes, $m \neq 0$, i.e.,

$$\Gamma_m = \Gamma_1, \qquad m = 2, 3, \cdots, n-1. \tag{30}$$

Thus, (29) gives

$$S_{ii} = n^{-1}[\Gamma_0 + (n-1)\Gamma_1], \tag{31a}$$

$$S_{ij} = n^{-1}[\Gamma_0 - \Gamma_1], \qquad i \neq j. \tag{31b}$$

These equations give the same results obtained in Refs. 2 to 8.

VII. THE FORK POWER DIVIDER

The conductance matrix, $\mathbf{G}_k$, of the kth isolation-resistor network of the fork power divider (Fig. 2c) is given by (1), with

$$\mathbf{M} = \begin{bmatrix} 1 & -1 & & & & & & & \\ -1 & 2 & -1 & & & & 0 & & \\ & -1 & 2 & & & & & & \\ & & & \cdot & \cdot & & & & \\ & & & & & \cdot & & & \\ & & & & & & \cdot & & \\ & & 0 & & & & & \cdot & \\ & & & & & & & 2 & -1 \\ & & & & & & & -1 & 1 \end{bmatrix} \tag{32}$$

It can be shown that $\mathbf{M}$ has the real orthonormal set of eigenvectors, $\mathbf{q}_m$, $m = 0, 1, \cdots, n-1$, where the ith entry, $i = 1, 2, \cdots, n$, of $\mathbf{q}_m$ is

$$q_{m,i} = \begin{cases} n^{-1/2}, & m = 0, \quad (33a) \\ (2/n)^{1/2}\cos[m(2i-1)\pi/2n], & m = 1, 2, \cdots, n-1. \quad (33b) \end{cases}$$

Note that (3) is satisfied. The corresponding eigenvalues are given, from (4), (32), and (33), by

$$\lambda_m = 4\sin^2(m\pi/2n), \qquad m = 0, 1, \cdots, n-1. \tag{34}$$

Note that (5) is satisfied.

A cross section of a microstrip circuit showing the planar, side-by-side arrangement of the n-conductor lines of the fork power divider is given in Fig. 4b. Pompei, Benevello, and Rivier[22] gave strong evidence, based on extensive numerical computations, that the capacitance matrices, $\mathbf{C}_k(x)$ and $\bar{\mathbf{C}}_k(x)$, of such a conductor arrangement have the same set of eigenvectors. However, for that set to be independent of k and x, and to coincide with the set defined in (33), i.e., to satisfy Assumptions 1 to 3 of Section II, the following conditions and approximations have to be fulfilled.

(*i*) The n conductors have the same PUL capacitance to ground, which is denoted by $C_{k,0}(x)$, or $\bar{C}_{k,0}(x)$, depending on the presence, or absence, respectively, of the dielectric substrate.

(*ii*) The PUL capacitances between adjacent conductors are identical and are given by $C_{k,1}(x)$, or $\bar{C}_{k,1}(x)$, depending on the presence, or absence, respectively, of the dielectric substrate.

(*iii*) The PUL capacitances between nonadjacent conductors are negligible.

Note that these conditions would, in general, require the conductors to have different widths and spacings. The two end conductors, in particular, would have to be narrower than the intermediate conductors, as depicted in Fig. 4b, to account for the fringing capacitances at both ends. Of course, all the conditions are fulfilled exactly for well-separated, i.e., uncoupled, identical conductors.

With the above three conditions in mind, one can write the PUL capacitance matrix of the conductors of Fig. 4b in the form

$$\mathbf{C}_k(x) = C_{k,0}(x)\mathbf{U} + C_{k,1}(x)\mathbf{M}, \tag{35}$$

where $\mathbf{U}$ is the $n \times n$ unity matrix and $\mathbf{M}$ is the same matrix given in (32). A similar expression holds for $\bar{\mathbf{C}}_k(x)$. Since any vector is an eigenvector of the unity matrix, it follows that $\mathbf{C}(x)$, $\bar{\mathbf{C}}_k(x)$, and $\mathbf{M}$ have the same set of eigenvectors defined in (33), i.e., that Assumptions 1 to 3 of Section II are satisfied. The eigenvalues of $\mathbf{C}_k(x)$ are given, from (2a) and (33) to (35), by

$$\eta_{k,m}(x) = C_{k,0}(x) + 4\sin^2(m\pi/2n)C_{k,1}(x), \; m = 0, 1, \cdots, n-1. \tag{36}$$

A similar expression holds for $\bar{\eta}_{k,m}(x)$.

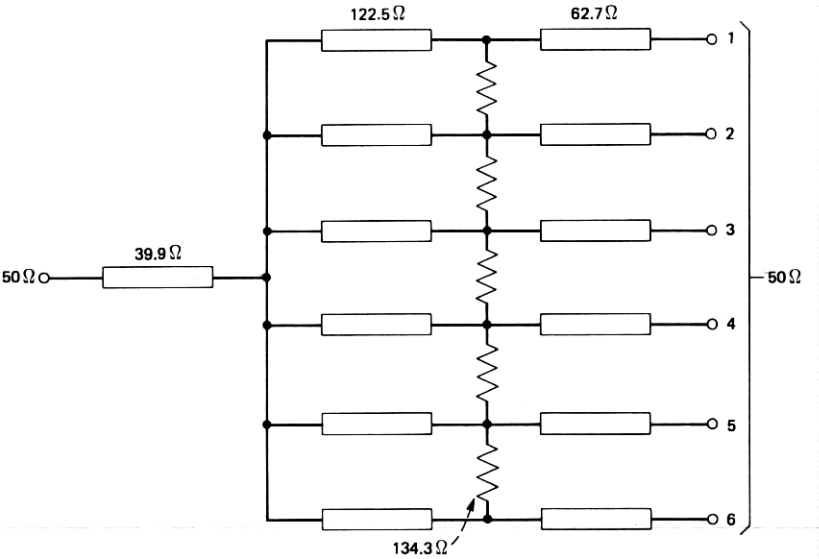

Fig. 5—The six-way, fork power divider with one stage of isolation resistors that is discussed in Example (a).

VIII. EXAMPLES

8.1 Example a

Consider the 6-way, fork power divider of Fig. 5, which consists of a one-stage input transformer, a one stage of 6-conductor lines and isolation-resistor network, and a one-stage transformer at each output port. All transmission lines are assumed to be uniform and uncoupled

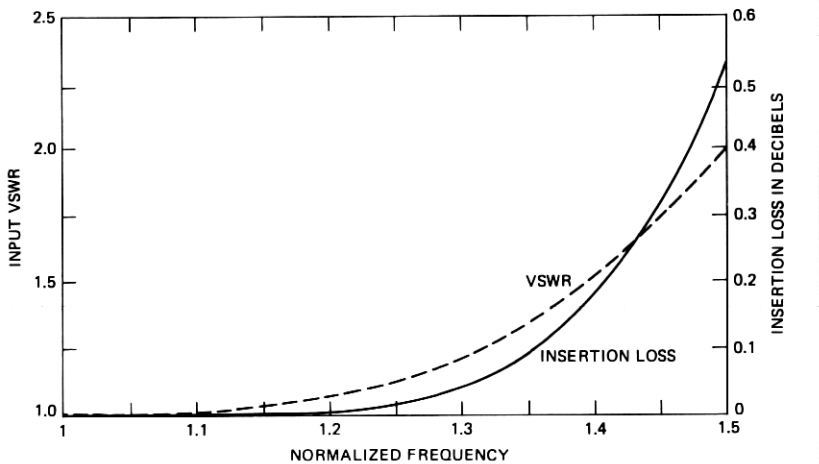

Fig. 6—The frequency responses of the input VSWR and the total insertion loss of the power dividers discussed in Examples (a), (b), and (c).

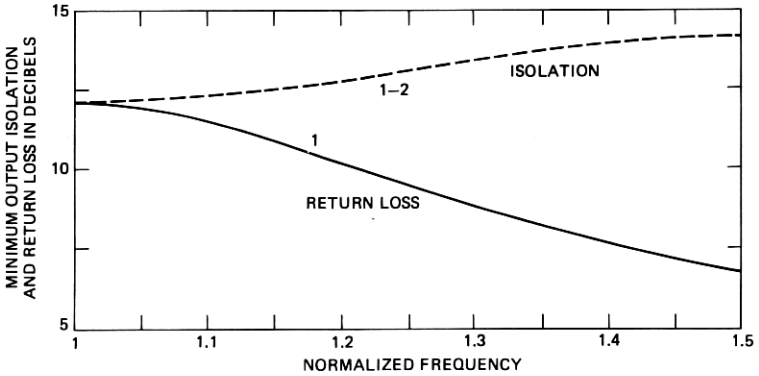

Fig. 7—The frequency responses of the minimum output return loss and minimum output isolation for the power divider discussed in Example (a). The numbers next to the curves correspond to the port numbers for which the return loss is minimum, or between which the isolation is minimum.

and to have quarter-wave lengths at band center. The characteristic impedances shown in the figure were calculated by applying the formulas of a maximally flat, homogeneous, 3-section, quarter-wave transformer [Ref. 20, eq. (6.04-2), p. 272] to the common-mode equivalent circuit of Fig. 3a. The value of each isolation resistance was calculated from Ref. 12, Table II, which gives an optimum value of 12.1 dB for the minimum output return loss and isolation at band center. The corresponding frequency responses of the input voltage standing-wave ratio (VSWR) and the total insertion loss are shown in Fig. 6. Figure 7 gives the corresponding minimum output return loss (solid line), and the minimum output isolation (dashed line). The numbers on the figure correspond to the port numbers for which the return loss is minimum, or between which the isolation is minimum.

8.2 Example b

A similar design procedure was used for the 6-way, fork power divider of Fig. 8, which consists of a one-stage input transformer, and two stages of 6-conductor lines and isolation-resistor networks. Note that the transmission lines are identical to those of Fig. 5. The values of the isolation resistances were calculated from Ref. 12, Table IV, which gives an optimum value of 21.3 dB for the minimum output return loss and isolation at band center. The frequency responses of these parameters are given in Fig. 9. Note the dramatic improvement in comparison to case (a). The frequency responses of the input VSWR and the total insertion loss are still given by Fig. 6.

8.3 Example c

To investigate the effects of coupling between adjacent conductors, consider the power divider of Fig. 8. Let the ratios of the PUL capaci-

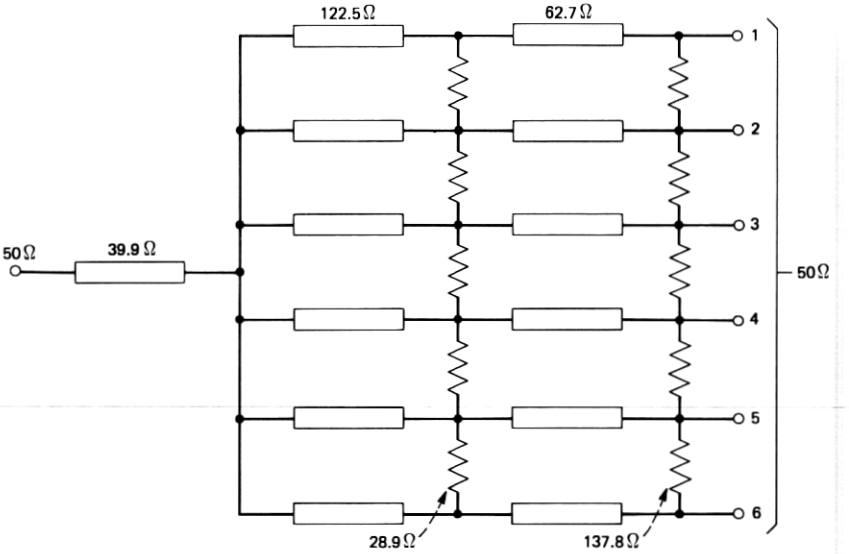

Fig. 8—The six-way, fork power divider with two stages of isolation resistors that is discussed in Examples (b) and (c).

tances (see Fig. 4b) be $C_{1,1}/C_{1,0} = \bar{C}_{1,1}/\bar{C}_{1,0} = 1$ for the first stage, which corresponds to fairly strong coupling, and $C_{2,1}/C_{2,0} = \bar{C}_{2,1}/\bar{C}_{2,0} = 0.25$ for the second stage, which corresponds to moderate coupling. The characteristic impedances shown in Fig. 8 are for the common mode.

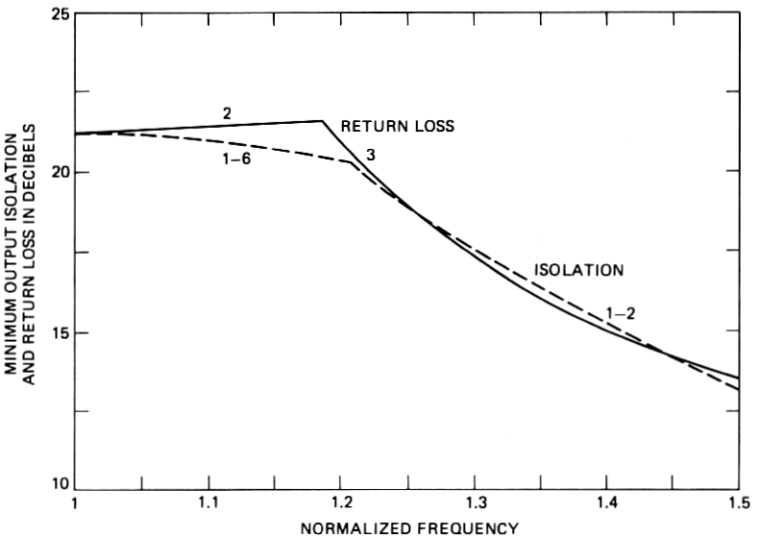

Fig. 9—The frequency responses of the minimum output return loss and minimum output isolation for the power divider discussed in Example (b).

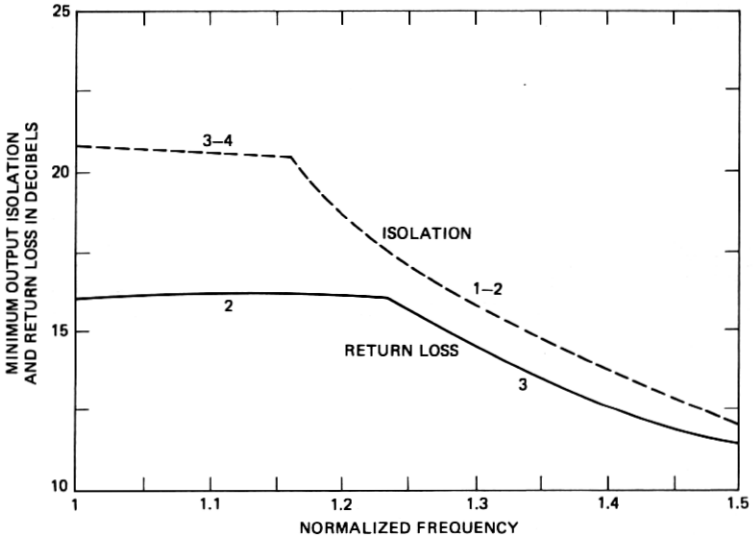

Fig. 10—The frequency responses of the minimum output return loss and minimum output isolation for the power divider discussed in Example (c).

The corresponding frequency responses of the minimum output return loss and minimum output isolation are given in Fig. 10. Note that the minimum output isolation (dashed line) is only slightly worse than that of case (b). On the other hand, the minimum output return loss (solid line), even though still excellent, dropped by about 5 dB near band center in comparison to that of case (b) (see Fig. 9). Presumably, some of that drop could be recovered by optimizing the values of the isolation resistances. This point, however, was not investigated. The frequency responses of the input VSWR and the total insertion loss are still given by Fig. 6.

IX. CONCLUSIONS

A unified theory has been presented for the computation of the frequency response of multi-stage, equi-amplitude, equi-phase, n-way power dividers of the Wilkinson, radial, and fork types. The n-conductor lines employed in these power dividers may consist of coupled or uncoupled, longitudinally uniform or nonuniform conductors in a transversely homogeneous or inhomogeneous dielectric medium. The theory reduces the analysis of the power divider to that of calculating the reflection and transmission coefficients of one lossless, two-port network, and $n - 1$, generally lossy, one-port networks. For circularly symmetric power dividers, such as the Wilkinson and the radial power dividers, the number of one-port networks that need to be considered reduces to only $[n/2]$, and for a Wilkinson power divider with uncou-

pled lines, to only one, as was done in Refs. 2 to 5. This method of analysis results in a considerable improvement on the speed of computation, as well as a sizable reduction in storage requirements, as compared to a standard method of nodal analysis. Furthermore, the aforementioned one- and two-port networks facilitate the design and optimization of the power dividers over a desired frequency band.

Note added in proof: The author was unaware of an excellent paper by Nagai, Maekawa, and Ono,[23] which is an expansion of their short paper of Ref. 14. The present paper duplicates some of their results. However, they only considered the case of uniform uncoupled lines.

REFERENCES

1. E. J. Wilkinson, "An *N*-Way Hybrid Power Divider," IRE Trans. Microwave Theory Tech., *MTT-8*, No. 1 (January 1960), pp. 116–118.
2. J. J. Taub and B. Fitzgerald, "A Note on *N*-Way Hybrid Power Dividers," IEEE Trans. Microwave Theory Tech., *MTT-12*, No. 2 (March 1964), pp. 260–261.
3. J. J. Taub and G. P. Kurpis, "A More General *N*-Way Hybrid Power Divider," IEEE Trans. Microwave Theory Tech., *MTT-17*, No. 7 (July 1969), pp. 406–408.
4. H. Y. Yee, F.-C. Chang, and N. F. Audeh, "*N*-Way TEM-Mode Broad-Band Power Dividers," IEEE Trans. Microwave Theory Tech., *MTT-18*, No. 10 (October 1970), pp. 682–688.
5. S. B. Cohn, "A Class of Broadband Three-Port TEM-Mode Hybrids," IEEE Trans. Microwave Theory Tech., *MTT-16*, No. 2 (February 1968), pp. 110–116.
6. R. B. Ekinge, "A New Method of Synthesizing Matched Broad-Band TEM-Mode Three-Ports," IEEE Trans. Microwave Theory Tech., *MTT-19*, No. 1 (January 1971), pp. 81–88.
7. R. P. Tetarenko and P. A. Goud, "Broad-Band Properties of a Class of TEM-Mode Hybrids," IEEE Trans. Microwave Theory Tech., *MTT-19*, No. 11 (November 1971), pp. 887–889.
8. N. Nagai and A. Matsumoto, "Basic Considerations on TEM-Mode Hybrid Power Dividers," 1973 IEEE International Microwave Symposium Digest, IEEE Cat. No. 73CH0736-9MTT (June 1973), pp. 218–220.
9. J. M. Schellenberg and M. Cohn, "A Wideband Radial Power Combiner for FET Amplifiers," 1978 IEEE ISSCC Digest, IEEE Cat. No. 78CH1298-9SSC (February 1978), pp. 164–165, 273.
10. M. Cohn, B. D. Geller, and J. M. Schellenberg, "A 10-Watt Broadband FET Combiner/Amplifier," 1979 IEEE International Microwave Symposium Digest, IEEE Cat. No. 79CH1439-9 MTT (April 1979), pp. 292–297.
11. K. J. Russell, "Microwave Power Combining Techniques," IEEE Trans. Microwave Theory Tech., *MTT-27*, No. 5 (May 1979), pp. 472–478, Fig. 11.
12. A. A. M. Saleh, "Planar, Electrically-Symmetric, *N*-Way, Hybrid Power Dividers/Combiners," IEEE Trans. Microwave Theory Tech., *MTT-28*, No. 6 (June 1980), pp. 555–563.
13. Z. Galani and S. J. Temple, "A Broadband *N*-Way Combiner/Divider," 1977 IEEE International Microwave Symposium Digest, IEEE Cat. No. 77CH1219-5MTT (June 1977), pp. 499–502.
14. N. Nagai, E. Maekawa, and K. Ono, "New *N*-Way Hybrid Power Dividers," 1977 IEEE International Microwave Symposium Digest, IEEE Cat. No. 77CH1219-5MTT (June 1977), pp. 503–504.
15. F.-Y. Chang, "Transient Analysis of Lossless Coupled Transmission Lines in a Nonhomogeneous Dielectric Medium," IEEE Trans. Microwave Theory Tech., *MTT-18*, No. 9 (September 1970), pp. 616–626.
16. H. E. Green, "The Numerical Solution of Some Important Transmission-Line Problems," IEEE Trans. Microwave Theory Tech., *MTT-13*, No. 5 (September 1965), pp. 676–692.
17. Y. M. Hill, N. O. Reckord, and D. R. Winner, "A General Method for Obtaining Impedance and Coupling Characteristics of Practical Microstrip and Triplate Transmission Line Configurations," IBM J. Res. Develop., *13* (May 1969), pp. 314–322.
18. W. T. Weeks, "Calculation of Coefficients of Capacitance of Multiconductor Trans-

mission Lines in the Presence of a Dielectric Interface," IEEE Trans. Microwave Theory Tech., *MTT-18*, No. 1 (January 1970), pp. 35–43.
19. N. Marcuvitz, *Waveguide Handbook*, MIT Rad. Lab Series, Vol. 10, New York: McGraw-Hill, 1948, pp. 29–47.
20. G. L. Matthaei, L. Young, and E. M. T. Jones, *Microwave Filters, Impedance-Matching Networks, and Coupling Structures,* New York: McGraw-Hill, 1964, pp. 26–45.
21. R. Bellman, *Introduction to Matrix Analysis,* New York: McGraw-Hill, 1970, pp. 242–243.
22. D. Pompei, O. Benevello, and E. Rivier, "Parallel Line Microstrip Filters in an Inhomogeneous Medium," IEEE Trans. Microwave Theory Tech., *MTT-26*, No. 4 (April 1978), pp. 231–238.
23. N. Nagai, E. Maekawa, and K. Ono, "New *N*-Way Hybrid Power Dividers," IEEE Trans. Microwave Theory Tech., *MTT-25*, No. 12 (December 1977), pp. 1008–1012.